Journal of Experimental Botany, Vol. 71, No. 3 pp. 970–985, 2020
doi:10.1093/jxb/erz468 Advance Access Publication October 23, 2019

RESEARCH PAPER

CIRCADIAN CLOCK ASSOCIATED 1 and ATAF2 differentially suppress cytochrome P450-mediated brassinosteroid inactivation

Hao Peng and Michael M. Neff*,

Department of Crop and Soil Sciences, Washington State University, Pullman, WA 99164, USA

* Correspondence: mmneff@wsu.edu

Received 1 November 2018; Editorial decision 10 October 2019; Accepted 15 October 2019

Editor: Richard Napier, University of Warwick, UK

Abstract

Brassinosteroids (BRs) are a group of steroid hormones regulating plant growth and development. Since BRs do not undergo transport among plant tissues, their metabolism is tightly regulated by transcription factors (TFs) and feedback loops. BAS1 (CYP734A1, formerly CYP72B1) and SOB7 (CYP72C1) are two BR-inactivating cytochrome P450s identified in *Arabidopsis thaliana*. We previously found that a TF ATAF2 (ANAC081) suppresses *BAS1* and *SOB7* expression by binding to the Evening Element (EE) and CIRCADIAN CLOCK ASSOCIATED 1 (CCA1)-binding site (CBS) on their promoters. Both the EE and CBS are known binding targets of the circadian regulatory protein CCA1. Here, we confirm that CCA1 binds the EE and CBS motifs on *BAS1* and *SOB7* promoters, respectively. Elevated accumulations of *BAS1* and *SOB7* transcripts in the *CCA1* null mutant *cca1-1* indicate that CCA1 is a repressor of their expression. When compared with either *cca1-1* or the *ATAF2* null mutant *ataf2-2*, the *cca1-1 ataf2-2* double mutant shows higher *SOB7* transcript accumulations and a stronger BR-insensitive phenotype of hypocotyl elongation in white light. CCA1 interacts with ATAF2 at both DNA–protein and protein–protein levels. *ATAF2*, *BAS1*, and *SOB7* are all circadian regulated with distinct expression patterns. These results demonstrate that CCA1 and ATAF2 differentially suppress *BAS1*- and *SOB7*-mediated BR inactivation.

Keywords: *Arabidopsis thaliana*, ATAF2, BAS1, brassinosteroids, CCA1, cytochrome P450, hypocotyl growth, SOB7, transcription factor.

Introduction

Brassinosteroids (BRs) are a class of polyhydroxysteroid hormones that regulate plant growth (J.Y. Zhu *et al.*, 2013), stress tolerance (Nolan *et al.*, 2017), and disease resistance (Belkhadir *et al.*, 2012). BRs do not undergo transport processes within the plant body (Symons and Reid, 2004; Savaldi-Goldstein *et al.*, 2007; Symons *et al.*, 2008). Their biosynthesis and catabolism are tightly regulated in different plant tissues and developmental stages (Zhao and Li, 2012). In the model plant *Arabidopsis thaliana*, several transcription factors (TFs) have been identified as regulators of the BR biosynthetic genes *DWARF4* (*DWF4*), *CONSTITUTIVE PHOTOMORPHOGENIC DWARF* (*CPD*), and *BRASSINOSTEROID-6-OXIDASE 2* (*BR6ox2*). A TCP-family TF TCP1 (Guo *et al.*, 2010) and a NAC-family TF JUNGBRUNNEN1 (JUB1) (Shahnejat-Bushehri *et al.*,

Abbreviations: 3-AT, 3-aminotriazole; BL, brassinolide; BR, brassinosteroid; CBS, CCA1-binding site; P450, cytochrome P450; EE, Evening Element; TF, transcription factor; Y1H, yeast one-hybrid; Y2H, yeast two-hybrid

2016) activate and suppress the expression of *DWF4*, respectively. COGWHEEL1 (COG1), a Dof-type TF, binds to the promoters of two phytochrome-interacting-factor (PIF)-encoding genes *PIF4* and *PIF5* to promote their expression (Wei *et al.*, 2017). PIF4 and PIF5 are two basic helix–loop–helix (bHLH) TFs that directly promote the expression of *DWF4* and *BR6ox2* (Wei *et al.*, 2017). Two homologous TFs CESTA (CES) and BR Enhanced Expression 1 (BEE1) interact with each other and promote the expression of *CPD* by directly binding a G-box motif in its promoter (Poppenberger *et al.*, 2011).

In Arabidopsis, the transcription of key BR biosynthetic and catabolic genes is feedback regulated to maintain hormone homeostasis (Tanaka *et al.*, 2005). PHYB ACTIVATION TAGGED SUPPRESSOR 1 (BAS1, CYP734A1, formerly CYP72B1) and SUPPRESSOR OF PHYB-4 7 (SOB7, CYP72C1) are two BR-inactivating cytochrome P450s (P450s) that are subject to transcriptional feedback regulation loops (Neff *et al.*, 1999; Turk *et al.*, 2003; 2005; Thornton *et al.*, 2010). Overexpression of *BAS1*, *SOB7*, or their orthologs from other plant species confers a BR-deficient dwarf phenotype in Arabidopsis (Neff *et al.*, 1999; Turk *et al.*, 2005; Thornton *et al.*, 2011).

Three TFs are known to be the transcriptional regulators of *BAS1* or *SOB7*. LATERAL ORGAN BOUNDARIES (LOB) directly binds the promoter of *BAS1* and activates its expression (Bell *et al.*, 2012). The auxin response factor 7 (ARF7) can bind to the E-box motifs of the *BAS1* promoter and suppress its expression (Youn *et al.*, 2016). We previously reported that the NAC TF ATAF2 (ANAC081) can bind to the promoters of both *BAS1* and *SOB7* as a repressor (Peng *et al.*, 2015). ATAF2 is also known to regulate disease resistance (Delessert *et al.*, 2005; X. Wang *et al.*, 2009; Wang and Culver, 2012), abiotic stress tolerance (Takasaki *et al.*, 2015), and auxin biosynthesis (Huh *et al.*, 2012). ATAF2 can act as either an activator or a repressor depending on growth conditions or promoter context (Delessert *et al.*, 2005; X. Wang *et al.*, 2009; Nagahage *et al.*, 2018).

ATAF2 binds the Evening Element (EE; AAAATATCT or its reverse complement sequence) and the CIRCADIAN CLOCK ASSOCIATED 1 (CCA1)-binding site (CBS; AAAAATCT or its reverse complement sequence) on *BAS1* and *SOB7* promoters (Peng *et al.*, 2015). The EE sequence has one extra 'T' when compared with that of the CBS, and both are known as the binding targets of the core circadian clock regulatory protein CCA1 (Wang and Tobin, 1998; Michael and McClung, 2002; Harmer and Kay, 2005). CCA1 is a MYB TF initially identified as an activator of *Lhcb1*3*, which encodes a light-harvesting Chl *a*/*b* protein (Wang *et al.*, 1997). Similar to ATAF2, CCA1 can act as either an activator (Fujiwara *et al.*, 2008) or a repressor (Li *et al.*, 2011) of downstream genes under different circumstances.

In this research, we confirmed that CCA1 binds the EE and CBS elements of *BAS1* and *SOB7* promoters, respectively. Like ATAF2, CCA1 is also a repressor of *BAS1* and *SOB7* expression. CCA1 interacts with ATAF2 at both DNA–protein and protein–protein levels. The suppressing effect of CCA1 and ATAF2 on *SOB7* expression can be either additive or redundant depending on the light or dark growth conditions for Arabidopsis seedlings. *ATAF2*, *BAS1*, and *SOB7* are all circadian regulated with distinct expression patterns. Our findings provide novel insight into the connection between BR homeostasis and circadian clock regulatory pathways.

Materials and methods

Plant materials and growth conditions

All Arabidopsis plants used in this study are in the Columbia (Col-0) background. The *cca1-1* mutant in the Col-0 background (CS67781) and the *ataf2-2* mutant (SALK_015750) were obtained from the Arabidopsis Biological Resource Center (ABRC). The *cca1-1* mutant in Col-0 was created by backcrossing the original *cca1-1* mutant in the Wassilewskija (Ws) background (Green and Tobin, 1999) six times into Col-0 (Yakir *et al.*, 2009). Primers for characterizing *cca1-1* were described previously (Green and Tobin, 1999). Primers for characterizing *ataf2-2* were designed using the web tool provided by the Salk Institute (http://signal.salk.edu/tdnaprimers.2.html). *cca1-1*, *ataf2-2*, and *cca1-1 ataf2-2* were all verified as gene knockout mutants via quantitative reverse transcription–PCR (qRT–PCR; see Supplementary Fig. S1 at *JXB* online). The p*BAS1*:BAS1-GUS and p*SOB7*:SOB7-GUS constructs and the histochemical β-glucuronidase (GUS) staining procedures were described previously (Sandhu *et al.*, 2012; Peng *et al.*, 2015). The p*ATAF2*::GUS construct harbors a transcriptional fusion of *GUS* and a 2 kb *ATAF2* promoter (X. Wang *et al.*, 2009). Plant GUS staining images were photographed using a Leica MZ10 F modular stereo microscope and a Leica DFC295 digital microscope color camera. For transgenic events, homozygous single-locus T-DNA insertion lines were selected for crossing and further analysis. Unless otherwise stated, all seeds were surface-sterilized by ethanol, plated on half-strength Linsmaier and Skoog medium with 10 g l^{-1} phytagel (Sigma-Aldrich, made in USA) and 15 g l^{-1} sucrose, stratified at 4 °C in the dark for 4 d, treated by red light for 1–2 h to induce germination, and grown in growth chambers at 25 °C in the dark, 80 μmol m^{-2} s^{-1} continuous white light (red:far-red light ratio 1:1), or 12 h 80 μmol m^{-2} s^{-1} light and a 12 h dark photoperiod depending on the experiment. Unless otherwise stated, 4-day-old seedlings were used for total RNA extraction and hypocotyl measurements. For circadian analysis of gene expression, seedlings were grown in a 12 h light and 12 h dark photoperiod for 7 d before RNA samples were extracted at 4 h intervals. Seedlings continued to grow in the same photoperiod during the 2 day RNA extraction schedule. For seed collection, seedlings were transferred to the greenhouse and grown at 22 °C in a photoperiod of 16 h of light and 8 h of dark. Seeds for all physiological and molecular assays are from plants grown at the same time under the same conditions.

Yeast one-hybrid and two-hybrid assays

The Gateway-compatible yeast one-hybrid (Y1H) system used in this research was developed by Deplancke *et al.* (2006). The promoter DNA fragments (baits) were amplified using primer pairs with adaptor sequences of the attB4 and attB1R sites, respectively (Deplancke *et al.*, 2004). The baits were cloned into pDONR-P4-P1R (Invitrogen) via BP reactions (Gateway BP Clonase II, Invitrogen). The resulting pDONR–bait constructs were used for LR reactions with Y1H destination vector pMW#2 (Gateway LR Clonase II, Invitrogen). pMW#2 contains the Gateway cassette of attR4 and attL1 recombination sites and a *HIS3* (pMW#2) reporter gene. The resulting pMW#2-bait constructs were linearized by digestion with *Xho*I. Then DNA bait::*HIS3* (pMW#2-bait) sequences were integrated via homologous recombination into the mutant *HIS3* locus of the yeast strain YM4271 developed for Y1H analysis. The successful integrations of baits in yeast genomes were verified by PCR using the combinations of bait- and vector-specific primers (Deplancke *et al.*, 2006). The self-activation of HIS3 was tested by yeast tolerance to gradient concentrations (0–80 mM) of

3-AT (3-aminotriazole; a competitive inhibitor of the His3p enzyme). After self-activation tests of HIS3 reporters, the yeast bait clones with the lowest background of reporter activity (self-activation) were selected and used to test their interactions with the preys. The sequences of baits p*BAS1*-EE, p*SOB7*-CBS, p*BAS1*-CBS1, p*BAS1*-EEm, and p*SOB7*-CBSm were described previously (Peng *et al.*, 2015). The sequence of bait p*ATAF2*-CBS is given in Supplementary Table S1. The full-length cDNA clone of *CCA1* (C105127; AT2G46830.2) was obtained from the ABRC. *CCA1* was cloned into the Gateway-compatible prey vector pACT2-GW (pACT2-GW-CCA1) and its interaction with the baits mentioned above was tested. An empty prey vector was used as a negative control. The procedure for the yeast two-hybrid (Y2H) assay was described previously (Zhao *et al.*, 2013). *ATAF2* cDNA was cloned into the Gateway-compatible bait vector pBTM116-D9 (pBTM116-D9-ATAF2). The prey construct pACT2-GW-CCA1 was used to transform yeast strain A. After testing for self-activation, the resulting clone was used for transformation of the bait construct pBTM116-D9-ATAF2. The empty bait vector was used as a negative control. The CCA1–ATAF2 interaction was tested by yeast tolerance to 3-AT and ability to grow in SDIV medium deprived of uracil, histidine, leucine, and tryptophan. The PCR-amplified sequences in all constructs used in this research were verified by sequencing.

EMSA and pull-down assay

Maltose-binding protein- (MBP) tagged CCA1 (MBP–CCA1), hexa-histidine-tagged CCA1 (His-CCA1), and hexa-histidine-tagged ATAF2 (His-ATAF2) were each expressed in the *Escherichia coli* strain Rosetta. All tags are fused at the N-terminus. *Escherichia coli* cell cultures were lysed via freeze–thaw followed by sonication in phosphate-buffered saline (PBS) containing lysozyme and Benzonase nuclease. MBP–CCA1 and MBP were purified using amylose resin (New England Biolabs). His-CCA1 and His-ATAF2 were purified using HisPur Ni-NTA resin (Thermo Fisher Scientific). To facilitate the successive binding experiments, maltose or imidazole was removed from purified MBP–CCA1, MBP, His-CCA1, or His-ATAF2 via four rounds of dialysis using the Slide-A-Lyzer mini dialysis device (Thermo Fisher Scientific). EMSA was carried out using the fluorescence-based EMSA kit from Invitrogen. DNA probes and protein–DNA complexes were separated by non-denaturing PAGE. DNA bands were stained by SYBR Green and scanned using the Bio-Rad ChemiDoc Touch imaging system. For the pull-down assay, the mixture of MBP–CCA1 and His-ATAF2 was incubated overnight at 4 °C with end over end mixing, and then loaded onto the amylose resin. After washing away unbound proteins, the bound proteins were eluted using elution buffer containing 10 mM maltose. As the negative control, the mixture of MBP and His-ATAF2 was subjected to identical procedures. The eluted samples were analyzed by SDS–PAGE and stained using Coomassie brilliant blue R-250.

Transcript analysis

Transcript accumulations of *BAS1*, *SOB7*, *ATAF2*, and *CCA1* were measured by qRT–PCR. Total RNA was extracted from 4-day-old seedlings using the RNeasy Plant Kit (Qiagen). The DNase I Digestion Set (Sigma) was used to perform on-column elimination of genomic DNA contamination. First-strand cDNA was synthesized using the iScript Reverse Transcription Supermix for RT-qPCR (Bio-Rad). Quantitative PCRs (qPCRs) were performed using the SsoAdvanced Universal SYBR Green Supermix (Bio-Rad) and the CFX96 Real-Time System (Bio-Rad). The Bio-Rad CFX Manager software was used to analyze and compare data using the $\Delta\Delta C_T$ method. Relative expression levels of target genes were determined by normalizing to the transcript levels of *POLYUBIQUITIN 10* (*UBQ10*). Each data point represents nine replicates (three biological replicates×three technical replicates). qPCR primers for *UBQ10*, *ATAF2*, *BAS1*, and *SOB7* were described previously (Peng *et al.*, 2015). qPCR primers for *CCA1* are 5'-TCGAAAGACGGGAAGTGGAACG-3' and 5'-GTCGATCTTCATTGGCCATCTCAG-3'. All qPCR primers were designed using QuantPrime (https://quantprime.mpimp-golm.mpg.de/; Arvidsson *et al.*, 2008).

Hypocotyl and root measurements

Seed plating and hypocotyl measurement were described previously (Favero *et al.*, 2016; 2017). For brassinolide (BL) treatment assays, seeds were put on BL-containing plates from the beginning of the experiments. The same volume of ethanol was used to dissolve gradient concentrations of BL and added to the media including the non-BL control. All 4-day-old seedlings were scanned/photographed and measured using NIH ImageJ (C.A. Schneider *et al.*, 2012). Each data point represents the result of the 30 tallest seedlings. Seven-day-old seedlings grown on vertical plates under continuous white light were used for primary root length measurement. Each data point represents the result of the 10 longest roots. All experiments were repeated three times. Each independent experiment showed a similar trend of differences.

Statistical analysis

One-way ANOVA with Tukey's HSD test was used to determine the significance of differences among multiple hypocotyl measurement or qPCR data sets. Two-tailed Student's *t*-test was used to compare two groups of qPCR data. The *P*-value significance level was set as 0.01.

Accession numbers

Arabidopsis Genome Initiative numbers for the genes used in this study are as follows: CCA1 (AT2G46830), ATAF2 (AT5G08790), BAS1 (AT2G26710), SOB7 (AT1G17060), and UBQ10 (AT4G05320).

Results

CCA1 binds the EE and CBS motifs on BAS1 *and* SOB7 *promoters, respectively*

ATAF2 binds three EE- and CBS-containing fragments of the *BAS1* and *SOB7* promoters (Fig. 1A), namely p*BAS1*-EE (−731 to −504), p*BAS1*-CBS1 (−844 to −786), and p*SOB7*-CBS (−1623 to −1524) (Peng *et al.*, 2015). Since both EE and CBS elements are known binding targets of CCA1 (Pan *et al.*, 2009), we tested, via targeted Y1H assays, the capability of CCA1 to bind to the three *BAS1* and *SOB7* promoter fragments mentioned above. CCA1 was confirmed to interact with p*BAS1*-EE (Fig. 1B) and p*SOB7*-CBS (Fig. 1C). Unlike ATAF2, CCA1 did not bind p*BAS1*-CBS1 in our assay (Fig. 1D).

Two EE/CBS-mutated fragments (Peng *et al.*, 2015), p*BAS1*-EEm (EE was mutated from AAAATATCT to AACATATCT) and p*SOB7*-CBSm (CBS was mutated from AGATTTTT to AGATTCTT), were used to test whether the interactions between CCA1 and p*BAS1*-EE/p*SOB7*-CBS were mediated by the EE and CBS motifs, respectively. Both p*BAS1*-EEm (Fig. 1E) and p*SOB7*-CBSm (Fig. 1F) lost their capacity to bind to CCA1 in targeted Y1H assays, indicating that the EE and CBS motifs are responsible for the binding of CCA1 to *BAS1* and *SOB7* promoters, respectively.

The binding of CCA1 to p*BAS1*-EE (Fig. 1G) and p*SOB7*-CBS (Fig. 1H) was further confirmed by EMSA. In our system, the MBP tag seemed to interfere with the capacity of CCA1 to bind to p*BAS1*-EE. Therefore, we showed the binding of His-CCA1 to p*BAS1*-EE instead (Fig. 1G). MBP cannot bind to p*BAS1*-EE (Fig. 1G), which indicated that the interaction between p*BAS1*-EE and CCA1 is protein selective. MBP–CCA1 can bind p*SOB7*-CBS whereas MBP cannot (Fig. 1H), which demonstrated that the specificity of binding comes from CCA1.

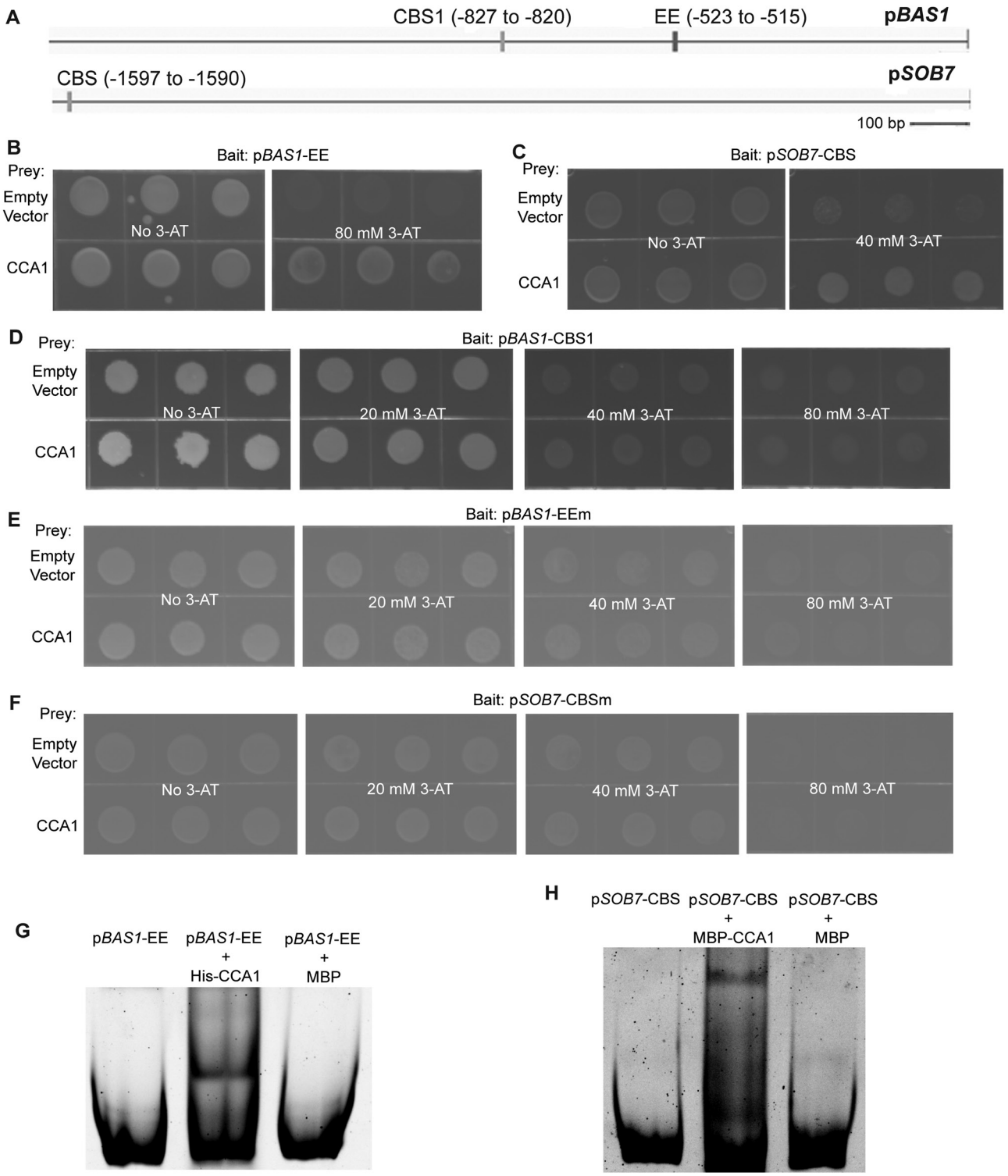

Fig. 1. CCA1 binds the EE and CBS motifs on *BAS1* and *SOB7* promoters, respectively. (A) The *BAS1* promoter harbors both EE and CBS motifs, while only one CBS motif exists in the *SOB7* promoter. CCA1 interacted with p*BAS1*-EE (B) and p*SOB7*-CBS (C), but not with p*BAS1*-CBS1 (D) in targeted Y1H assays. CCA1 did not interact with p*BAS1*-EEm (E) or p*SOB7*-CBS (F), in which the EE or CBS motifs have been mutated, respectively. Interactions of CCA1 with p*BAS1*-EEm (G) and p*SOB7*-CBS (H) were confirmed by EMSA. For each Y1H interaction tested, the indicated bait sequence was integrated into the mutant *HIS3* locus of the yeast strain YM4271. The bait-integrated yeast clone with the lowest self-activation was transformed with the indicated prey construct and empty prey vector (negative control), and then plated on selection medium supplemented with 3-AT at the concentrations shown. Yeast clones were grown at 28 °C for 3–4 d. Three independent clones were shown for each sample. For EMSA, His–CCA1 and MBP–CCA1 were incubated with p*BAS1*-EE and p*SOB7*-CBS, respectively, and separated by non-denaturing PAGE. DNA probes and protein–DNA complexes were stained by SYBR Green. MBP was used as a negative control.

CCA1 is a repressor of BAS1–GUS and SOB7–GUS activity

To test the effects of CCA1 on BAS1 and SOB7 activity, two constructs p*BAS1*:BAS1-GUS and p*SOB7*:SOB7-GUS (genomic DNA translational fusions with 1.6 kb and 2.1 kb of their native promoters, respectively; Sandhu *et al.*, 2012; Peng *et al.*, 2015) were used to transform the *CCA1* loss-of-function mutant *cca1-1*. Approximately 25% of the T_1 primary transformants of both p*BAS1*:BAS1-GUS/*cca1-1* (Fig. 2A) and p*SOB7*:SOB7-GUS/*cca1-1* (Fig. 2B) conferred a severe dwarf phenotype associated with BR deficiency (BR-dwarf). Similar BR-dwarf transformants were observed when expressing the two constructs in the *ATAF2* loss-of-function mutant *ataf2-2*, while none of the p*BAS1*:BAS1-GUS and p*SOB7*:SOB7-GUS transgenic plants in the Col-0 background showed dwarfism (Peng *et al.*, 2015). The results indicate that like ATAF2, CCA1 may also suppress the expression and activity of *BAS1* and *SOB7*.

To compare the activity of p*BAS1*:BAS1-GUS or p*SOB7*:SOB7-GUS in wild-type (Col-0) and *cca1-1* backgrounds with identical insertion sites in the Arabidopsis genome, we adopted a cross-segregation approach previously applied to *ataf2-2* (Peng *et al.*, 2015). Homozygous T_3 plants were isolated from the BR-dwarf p*BAS1*:BAS1-GUS/*cca1-1* and p*SOB7*:SOB7-GUS/*cca1-1* lines with T-DNA inserted at a single locus. Those homozygous T-DNA insertional plants were crossed with Col-0, and the F_2 segregants were genotyped. Many p*BAS1*:BAS1-GUS/*cca1-1* and p*SOB7*:SOB7-GUS/*cca1-1* F_2 segregants retained the BR-dwarf phenotype, whereas all p*BAS1*:BAS1-GUS/Col-0 and p*SOB7*:SOB7-GUS/Col-0 siblings were morphologically normal (Fig. 2C, D). F_3 homozygous segregants of p*BAS1*:BAS1-GUS/Col-0 (Fig. 2E), p*BAS1*:BAS1-GUS/*cca1-1* (Fig. 2E), p*SOB7*:SOB7-GUS/Col-0 (Fig. 2F), and p*SOB7*:SOB7-GUS/*cca1-1* (Fig. 2F) retained their morphologically normal or BR-dwarf phenotypes, respectively. The results confirmed that the BR-dwarf phenotype of p*BAS1*:BAS1-GUS/*cca1-1* and p*SOB7*:SOB7-GUS/*cca1-1* transgenic plants were caused by the disruption of CCA1.

CCA1 modulates the tissue-specific protein accumulation patterns of BAS1–GUS and SOB7–GUS

Both BAS1–GUS and SOB7–GUS have specific accumulation patterns that limit their presence in certain tissues of seedlings and plant organs (Sandhu *et al.*, 2012). BAS1–GUS accumulates in seedling roots, the shoot apex, and certain leaf regions, whereas SOB7–GUS activity can only be observed in the root tip and elongation zone (Peng *et al.*, 2015). Using CCA1–GUS transgenic lines, Pruneda-Paz *et al.* (2009) revealed that CCA1 exhibits expression throughout the whole seedling except the roots. Based on our previous results (Figs 1, 2), CCA1 may act as a tissue-specific repressor of BAS1 and SOB7. To test this hypothesis, we performed GUS staining on F_3 homozygous segregants of p*BAS1*:BAS1-GUS/Col-0, p*BAS1*:BAS1-GUS/*cca1-1*, p*SOB7*:SOB7-GUS/Col-0, and p*SOB7*:SOB7-GUS/*cca1-1* (Fig. 3; Supplementary Fig. S2). Five-day-old seedlings, cauline and rosette leaves, as well as flowers and siliques were stained (Fig. 3; Supplementary Fig. S2). To compare the effects of CCA1 and ATAF2 in modulating BAS1–GUS and SOB7–GUS accumulation, seedlings and flowers of corresponding F_3 homozygous segregants in Col-0 and *ataf2-2* backgrounds (Peng *et al.*, 2015) were also stained at the same time (Fig. 3). The results showed that BAS1 and SOB7 expression expanded to more tissues with the disruption of *CCA1*. In a *cca1-1* background, both BAS1–GUS and SOB7–GUS fusion signals were dramatically expanded and enhanced in seedlings, leaves, flowers, and siliques when compared with their expression patterns in the wild type (Col-0) (Fig. 3; Supplementary Fig. S2). Compared with CCA1, the disruption of ATAF2 led to even broader expression of BAS1–GUS and SOB7–GUS in seedlings and flowers (Fig. 3A–P).

CCA1 showed significantly reduced transcript accumulation in roots when compared with the rest of the seedling (Fig. 3Q), which is consistent with previous observations (Pruneda-Paz *et al.*, 2009). In contrast, *SOB7* was preferably expressed in seedling root (Fig. 3R). The relatively low expression of CCA1 in roots may at least partially allow *SOB7* to be expressed in these tissues. In contrast, the presence of CCA1 in other tissues may contribute to the inhibition of *SOB7* expression. Unlike CCA1, p*ATAF2*::GUS showed universal expression in seedlings (Supplementary Fig. 3S), which is consistent with the broad expansion of p*BAS1*:BAS1-GUS and p*SOB7*:SOB7-GUS in the *ataf2-2* genetic background (Peng *et al.*, 2015; Fig. 3D, H, L, P).

CCA1 and ATAF2 differentially suppress the transcript accumulation of BAS1 *and* SOB7

Since CCA1 and ATAF2 have similar functions in suppressing BAS1–GUS and SOB7–GUS accumulation, we made the *cca1-1 ataf2-2* double mutant and compared it with the single mutants and the wild type with regard to *BAS1* and *SOB7* transcript accumulation. For 4-day-old seedlings grown at 25 °C in 80 μmol m^{-2} s^{-1} continuous white light or darkness, *cca1-1*, *ataf2-2*, and the *cca1-1 ataf2-2* double mutant showed similarly elevated *BAS1* expression when compared with the wild type (Col-0) with the exception that *cca1-1 ataf2-2* showed lower *BAS1* transcript accumulation than either single mutant in the dark (Fig. 4A, B), demonstrating that the removal of either *CCA1* or *ATAF2* can significantly de-repress *BAS1* transcript accumulation. In contrast, in white light, the *cca1-1 ataf2-2* double mutant conferred significantly higher *SOB7* transcript accumulation than either *cca1-1* or *ataf2-2* single mutants (Fig. 4C). However, in darkness, the genetic impact of *CCA1* or *ATAF2* on *SOB7* transcript accumulation is similar and has no additive effect (Fig. 4D). These results indicate that CCA1 and ATAF2 can additively suppress *SOB7* transcript accumulation in white light but not in darkness.

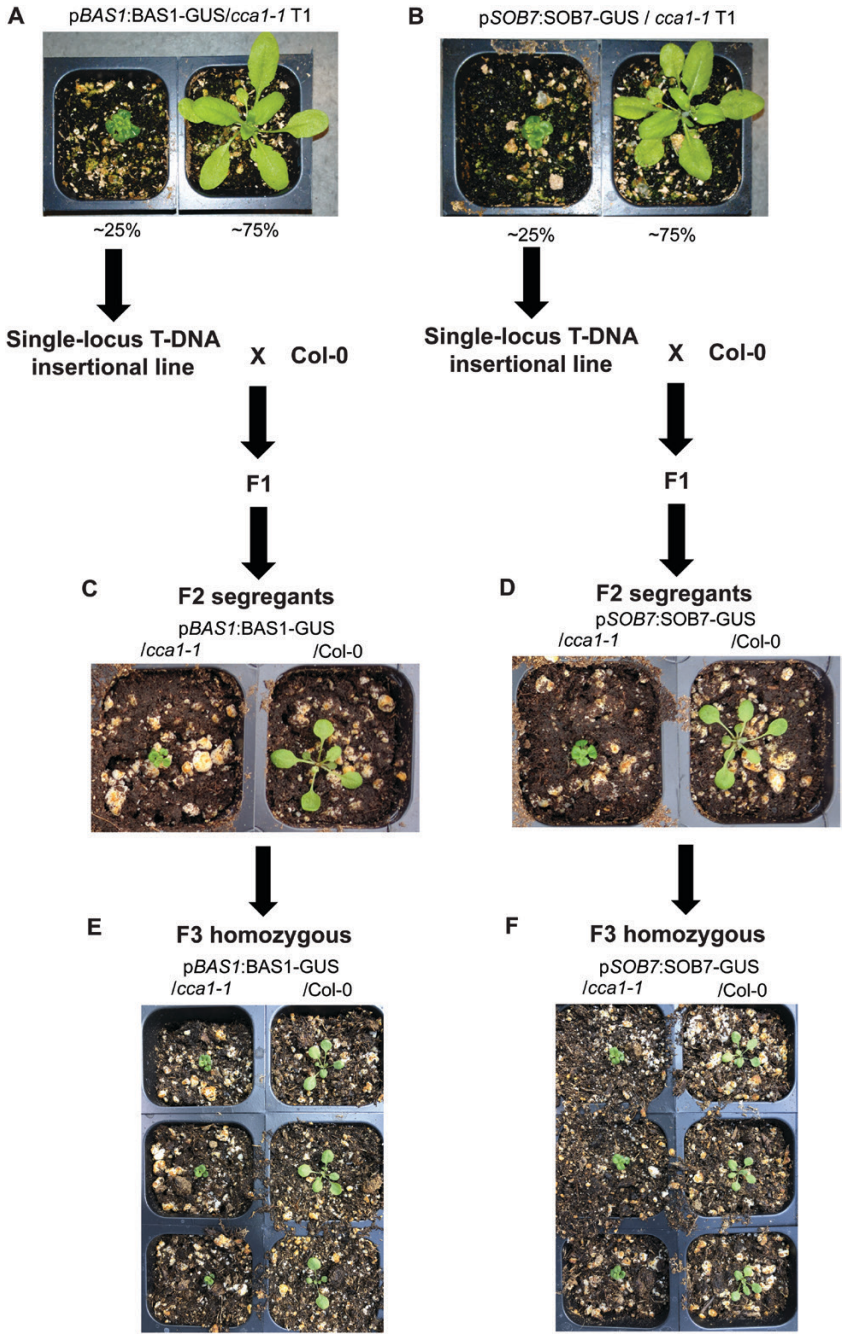

Fig. 2. CCA1 is a repressor of *BAS1* and *SOB7* expression. Ectopic expression of p*BAS1*:BAS1-GUS (A) and p*SOB7*:SOB7-GUS (B) in the *cca1-1* background caused BR deficiency-associated dwarfism in about a quarter of T_1 plants of both transgenic events. Single-locus T-DNA insertional p*BAS*1:BAS1-GUS/*cca1-1* and p*SOB7*:SOB7-GUS/*cca1-1* homozygous T_3 lines were selected from BR-dwarf plants and crossed with Col-0, respectively. Homozygous p*BAS*1:BAS1-GUS (C) and p*SOB7*:SOB7-GUS (D) sibling lines in *cca1-1* and Col-0 backgrounds were selected from the two F_2 segregation populations for comparison of morphology. F_3 homozygous segregants of p*BAS1*:BAS1-GUS/Col-0 (E), p*BAS1*:BAS1-GUS/*cca1-1* (E), p*SOB7*:SOB7-GUS/Col-0 (F), and p*SOB7*:SOB7-GUS/*cca1-1* (F) retained their morphologically normal or BR-dwarf phenotypes, respectively.

Both CCA1 and ATAF2 impact seedling responsiveness to exogenous BL and the BR biosynthesis inhibitor brassinazole

Since BRs promote hypocotyl growth in white light but have the opposite, suppressing, effect under darkness (Turk *et al.*, 2003; Peng *et al.*, 2015), Arabidopsis seedlings with elevated *BAS1* or *SOB7* expression are less responsive to exogenous BRs when compared with the wild type (Turk *et al.*, 2005; Peng *et al.*, 2015). To test the BR sensitivity of Col-0, *cca1-1*, *ataf2-2*, and *cca1-1 ataf2-2* seedlings of all four genotypes were grown on media with gradient concentrations of BL (0, 10, 100, and 1000 nM) for 4 d in 80 μmol m^{-2} s^{-1} of continuous white light, 12 h/12 h light and dark photoperiod, and darkness. Since *cca1-1* had slightly shorter hypocotyls than Col-0 even without BL treatment (Fig. 5A), seedling hypocotyl lengths in response to exogenous BL were described as percentage changes instead of their absolute values (Fig. 5B).

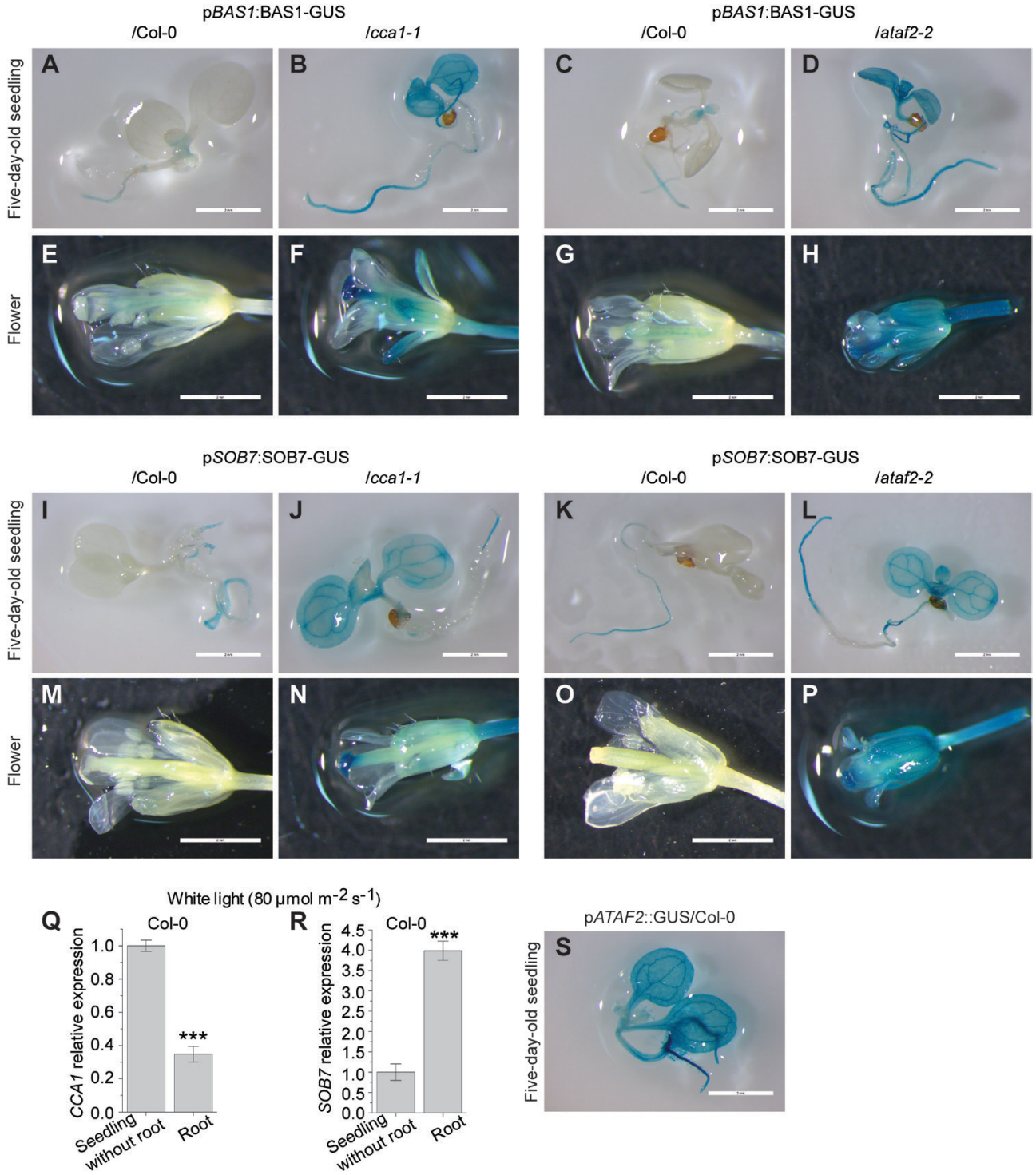

Fig. 3. CCA1 and ATAF2 modulate the tissue-specific expression patterns of BAS1 and SOB7 in seedlings and flowers. The roles of CCA1 and ATAF2 in restricting BAS1 and SOB7 expression within certain tissues of seedlings and flowers were demonstrated by GUS analysis on F_3 homozygous segregants of p*BAS1*:BAS1-GUS/Col-0 and p*BAS1*:BAS1-GUS/*cca1-1*, p*BAS1*:BAS1-GUS/Col-0 and p*BAS1*:BAS1-GUS/*ataf2-2*, p*SOB7*:SOB7-GUS/Col-0 and p*SOB7*:SOB7-GUS/*cca1-1*, and p*SOB7*:SOB7-GUS/Col-0 and p*SOB7*:SOB7-GUS/*ataf2-2* (A–P). (Q) *CCA1* showed significantly reduced transcript accumulation in seedling roots when compared with seedlings without roots. (R) *SOB7* was preferably expressed in seedling roots. Five-day-old seedlings grown at 25 °C in 80 µmol m^{-2} s^{-1} continuous white light were used for GUS staining and RNA extraction. Scale bars=2 cm. Each qRT–PCR value is the mean of results from three biological replicates×three technical replicates (n=9). Error bars denote the SE. Two-tailed Student's t-test was used to determine the significance of differences. ***P<0.001.

The hypocotyl growth of both *cca1-1* and *ataf2-2* was less responsive to BL treatments when compared with that of Col-0 (Fig. 5B). *cca1-1 ataf2-2* was even more insensitive to BL than the two single mutants (Fig. 5B). Based on our previous gene expression results (Fig. 4), the additive effect of CCA1 and ATAF2 in regulating BR-responsive hypocotyl

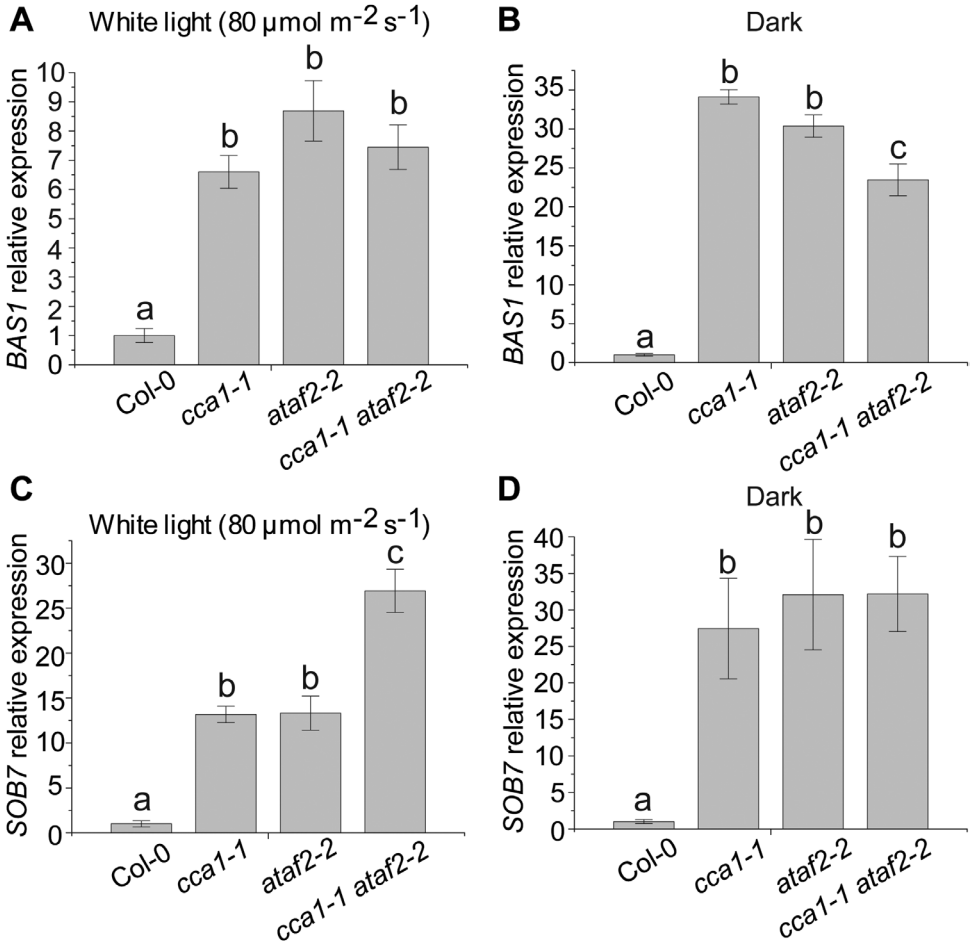

Fig. 4. CCA1 and ATAF2 differentially suppress the transcript accumulation of *BAS1* and *SOB7*. For 4-day-old seedlings grown at 25 °C in 80 μmol m^{-2} s^{-1} continuous white light (A) or darkness (B), *cca1-1*, *ataf2-2*, and the *cca1-1 ataf2-2* double mutant showed similarly elevated *BAS1* expression when compared with the wild type (Col-0) except that *cca1-1 ataf2-2* showed even lower *BAS1* transcript accumulation than either single mutant in the dark. In contrast, in white light, the *cca1-1 ataf2-2* double mutant conferred significantly higher *SOB7* transcript accumulation than either *cca1-1* or *ataf2-2* single mutants (C). However, in darkness, the genetic impact of *CCA1* or *ATAF2* on *SOB7* transcript accumulation is similar and has no additive effect (D). Each qRT–PCR value is the mean of results from three biological replicates×three technical replicates (n=9). Error bars denote the SE. One-way ANOVA with Tukey's HSD test was used to determine the significance of differences. Groups with significant differences were labeled by different letters.

growth in light is due to their collaborative suppression of *SOB7* expression. When seedlings were grown under the 12 h 80 μmol m^{-2} s^{-1} light and 12 h dark photoperiod (Fig. 5C), *cca1-1 ataf2-2* was less sensitive to BL than the two single mutants under 10 nM or 100 nM BL treatment (Fig. 5D). However, when under the toxic dose of 1000 nM BL treatment, *cca1-1 ataf2-2* and *ataf2-2* showed similar levels of BL insensitivity whereas *cca1-1* and Col-0 were almost equally sensitive to BL (Fig. 5D). In the dark, *cca1-1 ataf2-2* did not show higher BL insensitivity than either *cca1-1* or *ataf2-2* (Fig. 5E, F). The results indicated that compared with ATAF2, CCA1 may be more sensitive to dark and high-concentration BR conditions regarding its regulatory role in maintaining BR homeostasis.

With regard to root growth, *cca1-1 ataf2-2* seedlings had significantly shorter primary roots than Col-0, *cca1-1*, and *ataf2-2* (Fig. 5G). When testing the growth response of primary roots to the BR biosynthesis inhibitor brassinazole (BRZ; Asami *et al.*, 2000), *cca1-1*, *ataf2-2*, and *cca1-1 ataf2-2* all showed significantly higher sensitivity to exogenous BRZ treatments than Col-0, with *cca1-1 ataf2-2* being more sensitive than either single mutant with the treatment of 500 nM BRZ (Fig. 5H).

CCA1 is not feedback regulated by BRs

In addition to being a repressor of the BR-inactivating genes *BAS1* and *SOB7*, *ATAF2* is transcriptionally suppressed by exogenous BL, which forms a feedback regulatory loop (Peng *et al.*, 2015). This led to the hypothesis that *CCA1* may also be feedback regulated by exogenous BL. When treated with BL, *CCA1* transcript accumulation in Col-0 did not show any significant change (Fig. 6). The result indicated that unlike *ATAF2*, *CCA1* is not subject to BR-mediated transcriptional feedback regulation.

CCA1 interacts with ATAF2 at both the DNA–protein and protein–protein levels

Since CCA1 and ATAF2 share the same binding sites (the EE and CBS) (Peng *et al.*, 2015; Fig. 1), and both act as

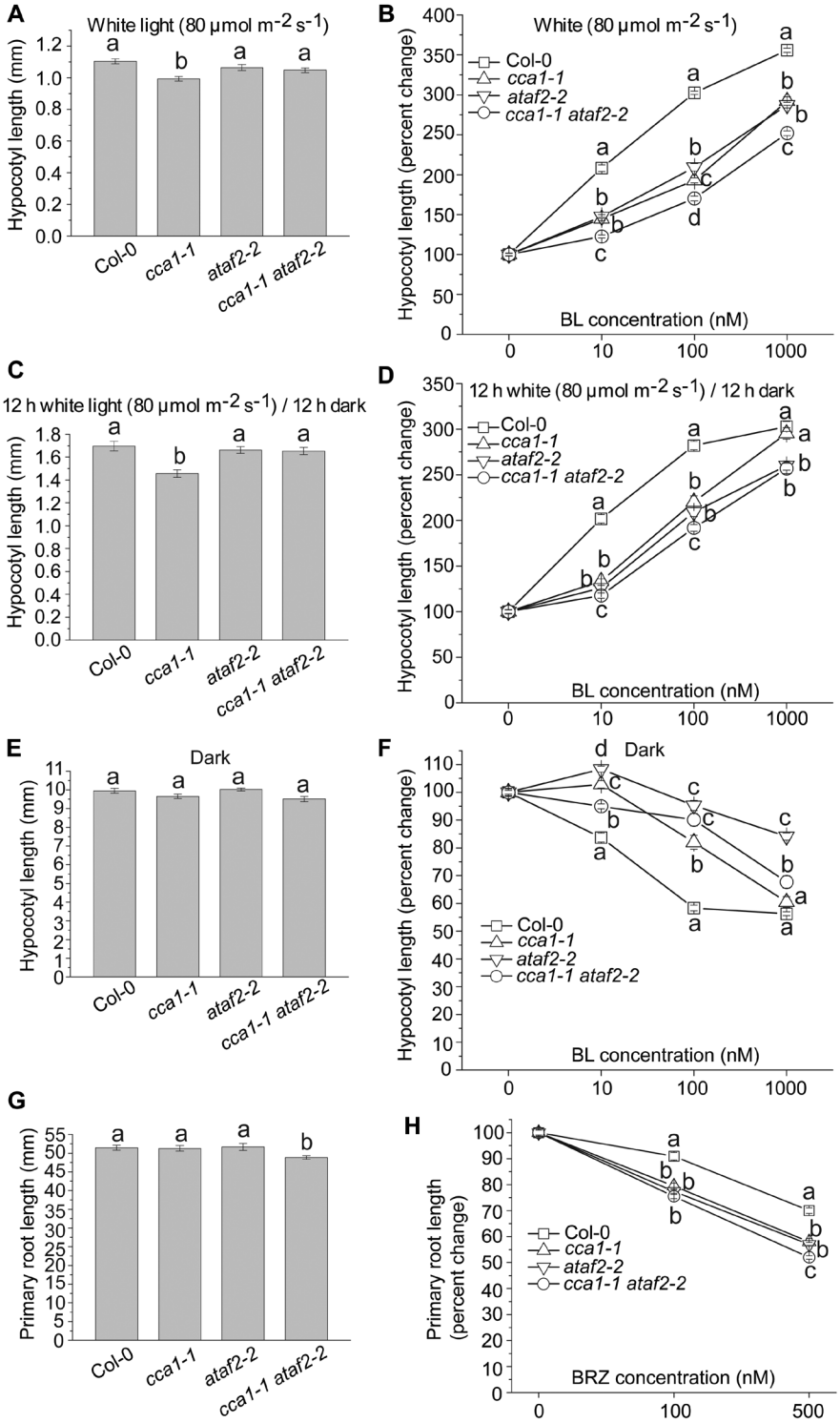

Fig. 5. Both *CCA1* and *ATAF2* impact seedling responsiveness to exogenous BL and the BR biosynthesis inhibitor BRZ. (A) *cca1-1* had slightly shorter hypocotyls than Col-0, *ataf2-2*, and *cca1-1 ataf2-2* when grown under continuous white light. (B) The hypocotyl growth of both *cca1-1* and *ataf2-2* was less responsive to BL treatments when compared with that of Col-0. *cca1-1 ataf2-2* was even more insensitive to BL than the two single mutants. When seedlings were grown under the 12 h 80 μmol m^{-2} s^{-1} light and 12 h dark photoperiod, *cca1-1* also had slightly shorter hypocotyls than Col-0, *ataf2-2*, and *cca1-1 ataf2-2* (C), and *cca1-1 ataf2-2* was more insensitive to BL than the two single mutants under 10 nM or 100 nM BL treatment (D). (E) *Col-0*, *cca1-1*, *ataf2-2*, and *cca1-1 ataf2-2* showed similar hypocotyl lengths when grown in the dark. (F) *cca1-1 ataf2-2* did not show higher BL insensitivity than either *cca1-1* or *ataf2-2* in the dark. (G) *cca1-1 ataf2-2* seedlings had slightly shorter primary roots than Col-0, *cca1-1*, and *ataf2-2*. (H) *cca1-1*, *ataf2-2*, and *cca1-1 ataf2-2* all showed significantly higher sensitivity to exogenous BRZ treatments than Col-0, with *cca1-1 ataf2-2* being even more sensitive than either single mutant with the treatment of 500 nM BRZ. Four-day-old seedlings grown at 25 °C in 80 μmol m^{-2} s^{-1} continuous white light, in a 12 h/12 h light/dark photoperiod, and in darkness were used for hypocotyl measurements. Each data point of hypocotyl length represents the average of measurements from 30 seedlings (n=30). Seven-day-old seedlings grown on vertical plates under continuous white light were used for primary root length measurement. Each data point of root length represents the result of 10 roots (n=10). Error bars denote the SE. One-way ANOVA with Tukey's HSD test was used to determine the significance of differences. Groups with significant differences were labeled by different letters.

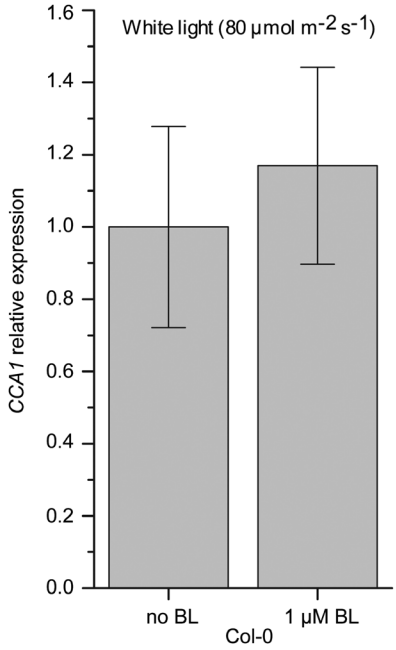

Fig. 6. *CCA1* is not feedback regulated by BRs. *CCA1* transcript accumulations in Col-0 did not show any significant change when treated with 1 µM BL. Four-day-old seedlings grown at 25 °C in 80 µmol m^{-2} s^{-1} continuous white light were used for RNA extraction. Each qRT–PCR value is the mean of results from three biological replicates×three technical replicates (n=9). Error bars denote the SE.

repressors of the BR-inactivating genes *BAS1* and *SOB7* (Peng *et al.*, 2015; Figs 2–4), we tested whether these two TFs genetically or physically interact. Like *BAS1* and *SOB7*, the *ATAF2* promoter also contains a CBS motif (−577 to −570; Fig. 7A), which is a potential binding target for CCA1. A 63 bp *ATAF2* promoter fragment, p*ATAF2*-CBS (−598 to −536; Supplementary Table S1), was used as the bait in a targeted Y1H assay to test its interaction with CCA1. CBS is the only predicted TF-binding site harbored by p*ATAF2*-CBS. The Y1H result demonstrates that CCA1 can bind to the promoter of *ATAF2* (Fig. 7B). Their interaction was further confirmed by EMSA (Fig. 7C). Compared with Col-0, *cca1-1* seedlings showed significantly higher *ATAF2* transcript accumulation when grown in continuous white light (Fig. 7D), whereas the opposite trend was observed in dark-grown seedlings (Fig. 7E). The results above reveal that CCA1 can act as either a repressor or an activator of *ATAF2* expression depending on the light conditions. On the other hand, no significant changes of *CCA1* expression in *ataf2-2* seedlings were observed in either continuous light (Supplementary Fig. S3A) or dark conditions (Supplementary Fig. S3B), which indicates that ATAF2 is not a transcriptional regulator of *CCA1*. Furthermore, CCA1 physically interacts with ATAF2 in a targeted Y2H assay (Fig. 7F). In a pull-down assay, MBP–CCA1 and His-ATAF2 can be eluted together from the amylose resin, whereas the resin only retained MBP from the mixture of MBP and His-ATAF2 (Fig. 7G). The pull-down result further confirmed physical interaction between CCA1 and ATAF2.

ATAF2, BAS1, *and* SOB7 *are all subject to circadian regulation*

Since CCA1 acts as a core regulator for the circadian clock (Wang and Tobin, 1998), we tested whether *ATAF2*, *BAS1*, and *SOB7* expression are circadian regulated in wild-type (Col-0) Arabidopsis seedlings (Fig. 8). After seedlings were grown in a 12 h/12 h light/dark cycle for 7 d, gene expression was monitored at 4 h intervals for 2 d under the same photoperiod setting. *CCA1* expression was used as a reference (Fig. 8A). Consistent with previous observations (Wang and Tobin, 1998), *CCA1* expression was largely stable, with the exception of peak levels occurring at dawn (Fig. 8A). *ATAF2*, *BAS1*, and *SOB7* were all circadian regulated with distinct expression patterns (Fig. 8B–D). Transcript accumulation of *ATAF2* kept decreasing in the dark period and began to increase after transiting to light (Fig. 8B). In contrast, both *BAS1* and *SOB7* showed higher expression levels in the dark than under light, and their transcript accumulation peaks appeared after entering the dark period for 4 h (Fig. 8C, D).

Discussion

BAS1, SOB7, *and multiple other BR-inactivating genes contribute to BR homeostasis*

BR inactivation can be achieved via multiple approaches in Arabidopsis, including hydroxylation (Neff *et al.*, 1999; Turk *et al.*, 2003), glycosylation (Poppenberger *et al.*, 2005; Husar *et al.*, 2011), acylation (Roh *et al.*, 2012; M. Wang *et al.*, 2012; K. Schneider *et al.*, 2012; Choi *et al.*, 2013; W. Zhu *et al.*, 2013; Zhang and Xu, 2018), and other unknown or unconfirmed mechanisms (Nakamura *et al.*, 2005; Takahashi *et al.*, 2005; Turk *et al.*, 2005; Marsolais *et al.*, 2007; Yuan *et al.*, 2007; Thornton *et al.*, 2010; Sandhu and Neff, 2013). At least 10 BR-inactivating genes have been identified in Arabidopsis including; P450 hydroxylases, glycosyltransferases, acyltransferases, sulfotransferases, and a reductase. The redundancy of BR-inactivating pathways is consistent with the fact that BRs act in local tissues at extremely low endogenous concentrations (He *et al.*, 2005; Kim *et al.*, 2006; Symons *et al.*, 2008). The role of catabolism in maintaining BR homeostasis appears to be as critical as the biosynthesis and signaling pathways, since tissue-specific BR levels can be fine-tuned by multiple inactivating enzymes and their upstream TF regulatory cascades. For example, LOB negatively regulates BR accumulation by activating *BAS1* expression at organ boundaries (Bell *et al.*, 2012). As two transcriptional repressors of *BAS1* and/or *SOB7*, ATAF2 and ARF7 integrate BR inactivation with auxin biosynthesis and signaling, seedling photomorphogenesis, disease resistance, and stress tolerance (Peng *et al.*, 2015; Youn *et al.*, 2016).

CCA1 is a direct repressor of both BAS1 *and* SOB7

The existence of EE and CBS motifs in *BAS1* and *SOB7* promoters (Peng *et al.*, 2015; Fig. 1A) indicates that these two genes may be included in the regulatory network of the core circadian

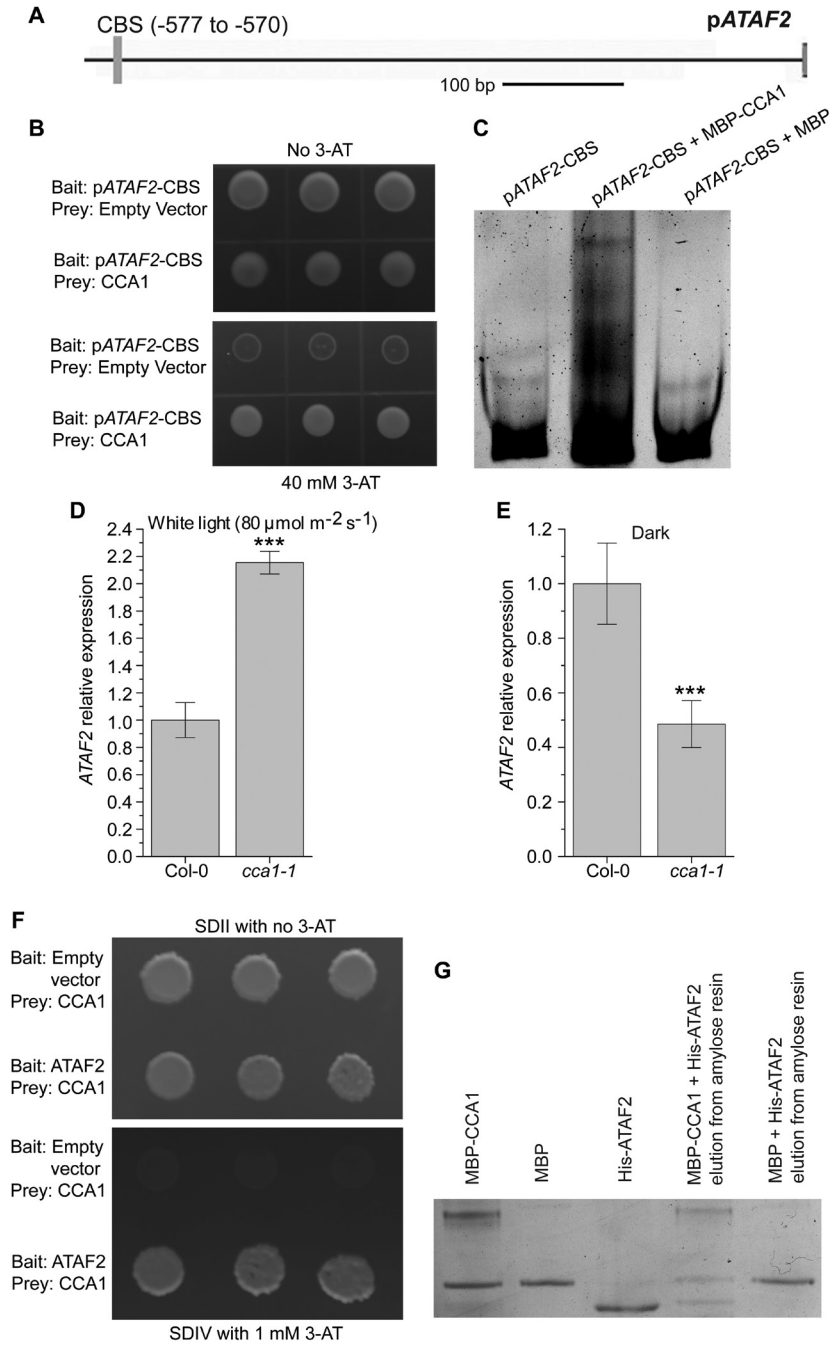

Fig. 7. CCA1 interacts with ATAF2 at both DNA–protein and protein–protein levels. (A) The *ATAF2* promoter contains a CBS motif. (B) CCA1 binds p*ATAF2*-CBS in a targeted Y1H assay. Their interaction was further confirmed by EMSA (C). Compared with Col-0, *cca1-1* seedlings showed significantly higher *ATAF2* transcript accumulation when grown in continuous white light (D), whereas the opposite trend was observed in dark-grown seedlings (E). (F) CCA1 physically interacts with ATAF2 in a targeted Y2H assay. (G) Physical interaction between CCA1 and ATAF2 was further confirmed by a pull-down assay. MBP–CCA1 and His-ATAF2 can be eluted together from the amylose resin whereas the resin only retained MBP from the mixture of MBP and His-ATAF2 (G). For Y1H assay, the p*ATAF2*-CBS bait was integrated into the mutant *HIS3* locus of the yeast strain YM4271. The bait-integrated yeast clone with the lowest self-activation was transformed with the CCA1 prey construct and empty prey vector (negative control). The interaction between CCA1 and p*ATAF2*-CBS was tested by yeast tolerance to 3-AT. For Y2H assay, the CCA1 prey construct was used to transform yeast strain A. After testing for self-activation, the resulting clone was used for transformation of the ATAF2 bait construct and the empty bait vector (negative control). The CCA1–ATAF2 interaction was tested by yeast tolerance to 3-AT and the ability to grown on SDIV medium. All yeast clones were grown at 28 °C for 3–4 d. Three independent clones are shown for each Y1H or Y2H sample. For EMSA, MBP–CCA1 was incubated with p*ATAF2*-CBS and separated by non-denaturing PAGE. The DNA probe and protein–DNA complex were stained by SYBR Green. MBP was used as a negative control. For the pull-down assay, MBP–CCA1 and His-ATAF2 were mixed and incubated overnight at 4 °C with end over end mixing, and then loaded onto the amylose resin. After washing away unbound proteins, the bound proteins were eluted using elution buffer containing 10 mM maltose. As the negative control, the mixture of MBP and His-ATAF2 went through identical procedures. The elution samples were analyzed by SDS–PAGE and stained using Coomassie brilliant blue R-250. Four-day-old seedlings grown at 25 °C in 80 μmol m^{-2} s^{-1} continuous white light were used for RNA extraction. Each qRT–PCR value is the mean of results from three biological replicates×three technical replicates (n=9). Error bars denote the SE. Two-tailed Student's t-test was used to determine the significance of differences. ***P<0.001.

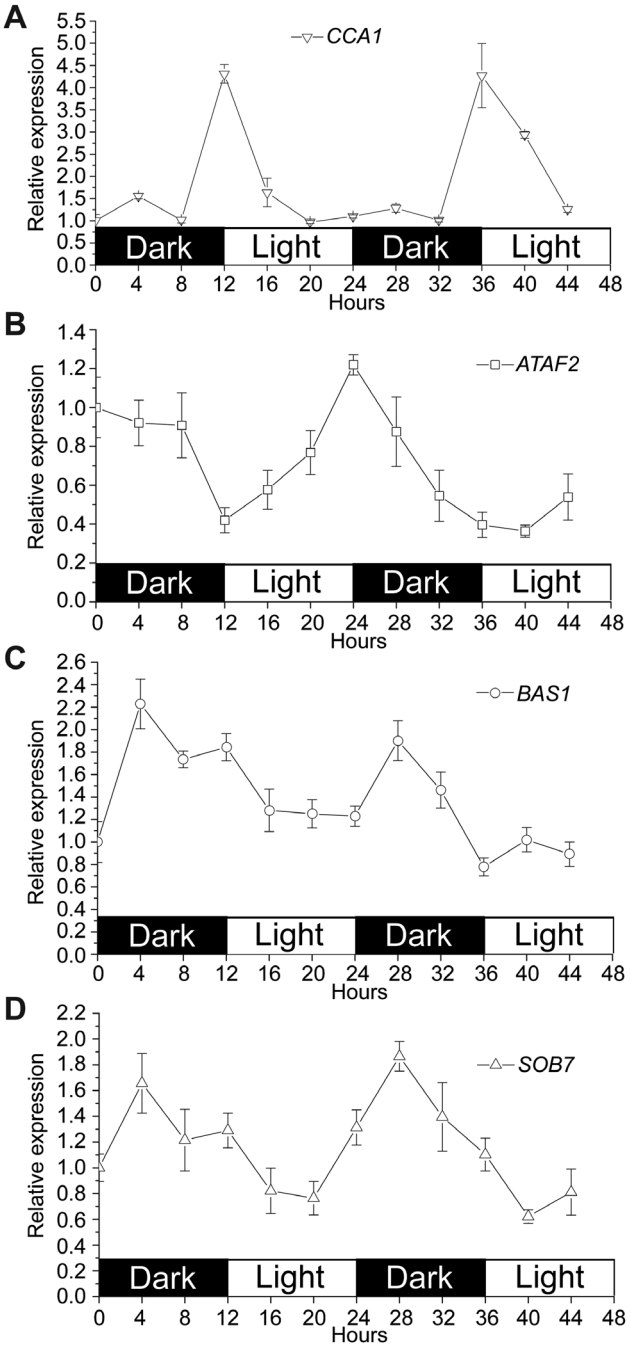

Fig. 8. *ATAF2*, *BAS1*, and *SOB7* are all circadian regulated with distinct expression patterns. (A) As a reference, *CCA1* expression was largely stable, with the exception of peak levels occurring at dawn. (B) Transcript accumulation of *ATAF2* kept decreasing in the dark period and began to increase after transiting to light. In contrast, both *BAS1* (C) and *SOB7* (D) showed higher expression levels in the dark than under light, and their transcript accumulation peaks appeared after entering the dark period for 4 h. After Col-0 seedlings were grown in a 12 h/12 h light/dark cycle for 7 d, gene expression was monitored at 4 h intervals for 2 d under the same photoperiod setting. Each qRT–PCR value is the mean of results from three biological replicates×three technical replicates (n=9). Error bars denote the SE.

clock protein CCA1. The genomic approach of ChIP-Seq did not identify *BAS1* or *SOB7* as a target of CCA1 (Nagel *et al.*, 2015; Kamioka *et al.*, 2016). However, our focused analysis demonstrated that CCA1 is a direct repressor of both *BAS1* and *SOB7* (Figs 1–4). Since P450s play critical roles in the metabolism of diverse secondary compounds, they have been used as reporters for different nodes in the circadian clock network (Pan *et al.*, 2009). Therefore, it is not surprising that both *BAS1* and *SOB7* are subject to the transcriptional regulation of CCA1. The lack of *BAS1* and *SOB7* in the genomic characterization of CCA1 targets can be explained by the inherent bias of the ChIP-Seq approach in enriching highly expressed loci (Teytelman *et al.*, 2013). The cause of this bias may be that DNA from actively transcribed regions tends to be more exposed to binding proteins and antibodies due to nucleosome depletion (Teytelman *et al.*, 2013). Since both *BAS1* and *SOB7* have extremely low expression levels that are restricted to specific tissues (Neff *et al.*, 1999; Turk *et al.*, 2003, 2005; Sandhu *et al.*, 2012; Peng *et al.*, 2015), the two genes are more likely to be filtered out than other loci in the ChIP-Seq assay.

CCA1 regulates multiple BR signaling and metabolic genes

There have been established associations between CCA1 and BRs. Two TF-encoding genes involved in BR signaling, *ATBS1 (ACTIVATION-TAGGED BRI1 SUPPRESSOR 1)-INTERACTING FACTOR 1* (*AIF1*; H. Wang *et al.*, 2009) and *MYB-LIKE 2* (*MYBL2*; Ye *et al.*, 2012), have been identified by both Nagel *et al.* (2015) and Kamioka *et al.* (2016) as direct targets of CCA1. CCA1 also binds to the promoter of the BR biosynthetic gene *DWF4* and activates its expression (Zheng *et al.*, 2018). This report, together with our finding that CCA1 directly suppresses the BR-inactivating genes *BAS1* and *SOB7* (Figs 1–4), suggests that CCA1 is an overall positive regulator of BR accumulation.

CCA1 is selective in binding EE and CBS elements

Although EEs and CBSs are confirmed binding motifs for CCA1, CCA1 does not associate with all of the EEs or CBSs in the Arabidopsis genome (Kamioka *et al.*, 2016). This binding may require appropriate sequence context within the broader regulatory region (Kamioka *et al.*, 2016). CCA1 also prefers to bind EEs relative to CBSs (Nagel *et al.*, 2015; Kamioka *et al.*, 2016). Consistent with these findings, CCA1 did not bind p*BAS1*-CBS1, but did interact with p*BAS1*-EE in our study (Fig. 1B, D, E, G). In contrast, ATAF2 is able to bind both p*BAS1*-EE and p*BAS1*-CBS1 (Peng *et al.*, 2015).

CCA1 and ATAF2 have overlapping and distinct patterns in suppressing BAS1 *and* SOB7

Disruption of either *ATAF2* (Peng *et al.*, 2015) or *CCA1* (Fig. 3A–T) led to the expansion of BAS1 and SOB7 expression to additional tissues, but the suppressing patterns of CCA1 and ATAF2 are not identical. Compared with *CCA1*, *ATAF2* disruption caused an enhanced expansion of BAS1 and SOB7 in seedlings and flowers (Fig. 3A–P). These tissue-specific pattern differences may reflect the distinct expression patterns of CCA1 and ATAF2 (Fig. 3Q, S).

About a quarter of the T_1 p*BAS1*:BAS1-GUS/*cca1-1* (Fig. 2A) and p*SOB7*:SOB7-GUS/*cca1-1* (Fig. 2B) transformants showed the BR-dwarf phenotype. Similar BR-dwarfs were previously observed in p*BAS1*:BAS1-GUS/*ataf2-2* and p*SOB7*:SOB7-GUS/*ataf2-2* transformants (Peng *et al.*, 2015). However, there is no visible dwarfism in *cca1-1*, *ataf2-2*, or the *cca1-1 ataf2-2* double mutant. Since GUS translational fusions can increases protein stability in Arabidopsis (Chae *et al.*, 2012; Spartz *et al.*, 2012), BAS1–GUS and SOB7–GUS may be more likely to confer BR-dwarfing than their native forms in the *cca1-1* and/or *ataf2-2* mutant backgrounds. There are also other factors that may contribute to the BR-dwarf phenotype observed in p*BAS1*:BAS1-GUS and *SOB7*:SOB7-GUS transgenic plants in the *cca1-1* and/or *ataf2-2* mutant background. There is an additional *BAS1* or *SOB7* copy from the original Arabidopsis genome in each transgenic plant, which can result in higher *BAS1* or *SOB7* expression. Depending on the insert location of the transgene, adjacent enhancer elements may increase gene expression. Some of the remote suppressing *cis*-regulatory elements may not be included in the p*BAS1*:BAS1-GUS and p*SOB7*:SOB7-GUS constructs. An increase of *BAS1* or *SOB7* expression caused by all these factors may not be sufficient to induce the BR-dwarf phenotype in transgenic plants in the Col-0 background but can lead to dwarfism in the *cca1-1* and/or *ataf2-2* mutant backgrounds. In contrast, none of the four factors mentioned above exists in the original *cca1-1*, *ataf2-2*, or *cca1-1 ataf2-2* genetic backgrounds.

CCA1 and ATAF2 additively suppress SOB7 *expression in white light*

In both light- and dark-grown seedlings, CCA1 and ATAF2 suppress *BAS1* expression without an additive effect (Fig. 4A, B). In contrast, CCA1 and ATAF2 additively suppress *SOB7* expression in seedlings grown in continuous white light (Fig. 4C). However, suppression of *SOB7* expression by CCA1 and ATAF2 is not additive in darkness (Fig. 4D). This light-dependent collaborative suppression of *SOB7* helps to explain the observation that *cca1-1 ataf2-2* seedlings only show greater insensitivity to exogenous BL treatments than either of the single mutants when grown in white light but not in darkness (Fig. 5A–F). Although BL is not likely to be a preferred substrate for SOB7 (Thornton, *et al.*, 2010), increased expression of SOB7 can still reduce the overall endogenous levels of BRs. It is important to note that the differential regulatory patterns on *BAS1* and *SOB7* expression are probably influenced by the binding of CCA1 and ATAF2 (Peng *et al.*, 2015; Fig. 1), light- and tissue-specific regulation of *CCA1* and *ATAF2* expression (Wang and Tobin, 1998; Peng *et al.*, 2015; Fig. 8), and CCA1–ATAF2 interactions at both the DNA–protein and protein–protein levels (Fig. 7). Though we have shown that CCA1 and ATAF2 physically interact via targeted Y2H analysis and the pull-down assay (Fig. 7F, G), attempts to test their *in planta* interaction via bimolecular fluorescence complementation did not generate positive results. Thus, CCA1–ATAF2 physical interactions *in planta* may be transient, tissue specific, or require post-translational modification of either protein. In the dark, *cca1-1 ataf2-2* showed slightly but significantly lower *BAS1* transcript accumulation than either single mutant (Fig. 4B). It is possible that CCA1 and ATAF2 forms a heterodimer to suppress *BAS1* expression in the dark. Disruption of either protein abolishes the suppression effect, but the protein left can still bind to the *BAS1* promoter to prevent potential binding of other TFs on the same site. When both CCA1 and ATAF2 are disrupted, they lose the transcriptional suppression effect as well as the ability of DNA to bind to the *BAS1* promoter. The binding of additional repressors may lead to decreased *BAS1* expression in *cca1-1 ataf2-2* when compared with either single mutant.

Light and BRs have complex effects on CCA1's role in BR homeostasis

As part of a feedback regulation loop, *ATAF2* expression can be suppressed by external BL treatments (Peng *et al.*, 2015). Additionally, microarray data showed that three other members of the *ATAF* subfamily, *ATAF1* (*ANAC002*), *ANAC102*, and *ANAC032*, are also transcriptionally down-regulated by BL (Kleinow *et al.*, 2009). In contrast, CCA1 is not feedback regulated by BL in our study (Fig. 6). Since CCA1 is a core regulator for the circadian clock, it is not surprising that BRs do not have a significant impact on its expression. With the treatment of 1000 nM BL, *cca1-1* and Col-0 showed similar BL response phenotypes when grown under darkness or a 12 h/12 h light/dark photoperiod, but *cca1-1* was still more insensitive to BL than Col-0 under continuous light (Fig. 5A–F). This observation indicates that high concentrations of BRs together with darkness may attenuate CCA1's function in maintaining BR homeostasis, which is consistent with the primary role of CCA1 in circadian regulation and the previous observation that *CCA1* is transcriptionally induced by light (Wang and Tobin, 1998).

The circadian oscillation pattern of ATAF2 *is different from that of* BAS1 *and* SOB7

BAS1 and *SOB7* have a similar circadian oscillation pattern that shows higher expression in the dark, whereas *ATAF2*'s oscillation cycle is largely opposite, with expression decreasing in the dark and increasing in the light period (Fig. 8B–D). This observation is consistent with our previous finding that ATAF2 is a repressor for *BAS1* and *SOB7* expression (Peng *et al.*, 2015). The expression of *CCA1* itself is also subject to circadian oscillation, with peak levels occurring at dawn (Fig. 8A). With the exception of the dawn period, *CCA1* expression levels are relatively low and stable (Fig. 8A). The circadian oscillation pattern of *CCA1* is largely consistent with our observation that CCA1 suppresses *ATAF2* expression in the light but the effect switches to promotion in darkness (Fig. 7C, D). The comparison of oscillation patterns between *CCA1* and *BAS1/SOB7* (Fig. 8A, C, D) also largely supports our observation that CCA1 is a repressor of *BAS1* and *SOB7* expression (Figs 2–4). Peak *CCA1* expression levels appear when plants enter the light photoperiod (Fig. 8A). In contrast, both *BAS1* and *SOB7* have peak expression levels after entering the dark photoperiod for 4 h, and they both have generally

lower transcript accumulations during the light photoperiod (Fig. 8C, D). Although both CCA1 and ATAF2 are repressors of *BAS1* and *SOB7*, the circadian oscillation pattern of *ATAF2* is different from that of *CCA1* (Fig. 8A, B). *CCA1* expression can be immediately induced by light, but the effect of light switches to suppression after 1 h (Wang and Tobin, 1998). In contrast, light consistently promotes *ATAF2* expression during the whole light photoperiod (Fig. 8B). Unlike *CCA1* showing higher accumulation only during the dawn period (Fig. 8A), *ATAF2* has opposite expression patterns with similar patterns in light and dark photoperiods (Fig. 8B). Despite the overall consistency between the circadian oscillation patterns and the suppression/activation relationships of *CCA1*, *ATAF2*, *BAS1*, and *SOB7*, there are still discrepancies during some time periods. These discrepancies can be explained by the fact that the circadian clock is regulated by multiple players besides CCA1, such as CCA1's closely related partner LATE ELONGATED HYPOCOTYL (LHY; Schaffer *et al.*, 1998).

Light regulates ATAF2 *expression via either the circadian or the photomorphogenic pathway*

In seedlings grown under a 12 h light and 12 h dark photoperiod, *ATAF2* expression gradually drops in the dark and increases steadily after the transition to light, with transcript accumulation levels peaking at the beginning of the evening and being the lowest around dawn (Fig. 8B). On the other hand, we previously found that *ATAF2* has higher transcript accumulation in dark-grown etiolated seedlings than in seedlings grown under continuous white light, and that the expression of *ATAF2* in white light is fluence rate dependent (Peng *et al.*, 2015). *ATAF2* expression can also be suppressed when etiolated seedlings are transferred to white light (Peng *et al.*, 2015). These results indicate that *ATAF2* is transcriptionally regulated by light via either the circadian or the photomorphogenic pathway. When seedlings are grown under a light/dark circadian photoperiod, *ATAF2* expression is induced during the light period. In contrast, ATAF2 has higher transcript accumulation in seedlings undergoing skotomorphogenesis than in photomorphogenic seedlings.

Current model

We summarized the roles of CCA1 and ATAF2 in regulating BR inactivation and how circadian and photomorphogenic pathways are incorporated (Fig. 9). Both CCA1 and ATAF2 suppress the expression of the BR-inactivating genes *BAS1* and *SOB7* via direct binding to their promoters. However, the role of CCA1 and ATAF2 with regard to BR inactivation is dynamic with respect to the light environment. Both *BAS1* and *SOB7* are circadian regulated, with higher expression in the dark period. Transcriptionally induced by light, *CCA1* plays a role in the oscillation of *BAS1* and *SOB7*. While *ATAF2* expression is feedback suppressed by BRs, *CCA1* is not subject to this transcriptional regulation. CCA1 suppresses *ATAF2* expression in seedlings grown under light but switches to an activator for *ATAF2* in etiolated seedlings. In addition, CCA1 may also physically interact with ATAF2 at the protein level. It is important to point out, however, that this model only focuses on the components characterized in this study. Clearly, other CCA1- and ATAF2-interacting proteins, as well as additional regulatory TFs, are likely to have an impact on the overall regulation of the BR-inactivating genes *BAS1* and *SOB7*.

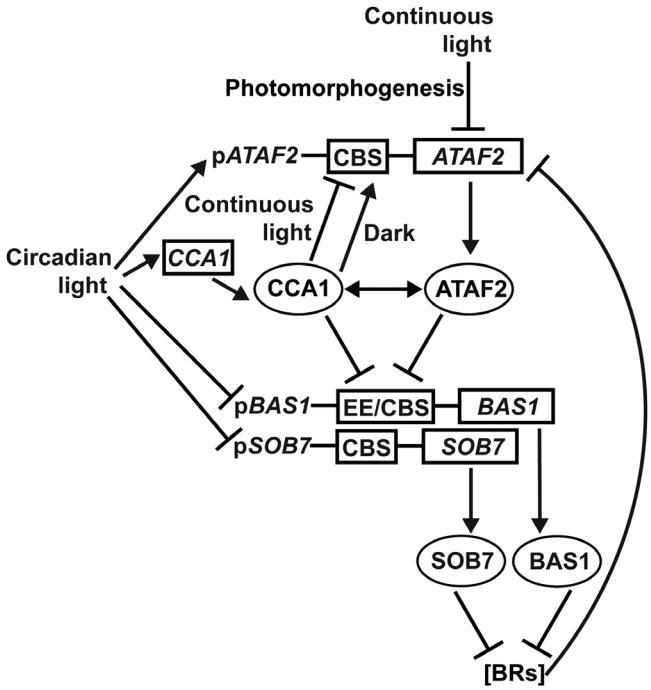

Fig. 9. Model for the roles of CCA1 and ATAF2 in regulating BR inactivation and the incorporation of circadian and photomorphogenic pathways. Both CCA1 and ATAF2 suppress the expression of BR-inactivating genes *BAS1* and *SOB7* via direct binding to their promoters. BRs promote Arabidopsis hypocotyl growth under light. BAS1 and SOB7 inhibit hypocotyl elongation by catabolizing BRs. Both *BAS1* and *SOB7* are circadian regulated with higher expression in the dark period. Transcriptionally induced by light, *CCA1* plays a role in the oscillation of *BAS1* and *SOB7*. While *ATAF2* expression is feedback suppressed by BRs, *CCA1* is not subject to such transcriptional regulation. CCA1 suppresses *ATAF2* expression in seedlings grown under light but switches to an activator for *ATAF2* in etiolated seedlings. CCA1 can also physically interact with ATAF2 at the protein level. Light induces *ATAF2* expression in seedlings undergoing a circadian photoperiod but acts as a repressor when seedlings transit from skotomorphogenesis to photomorphogenesis.

Supplementary data

Supplementary data are available at *JXB* online.

Table S1. Sequence of the *ATAF2* promoter fragment used for targeted Y1H.

Fig. S1. qRT–PCR assays on *CCA1* and *ATAF2* transcript accumulations demonstrate that *cca1-1*, *ataf2-2*, and *cca1-1 ataf2-2* are all gene knockout mutants.

Fig. S2. CCA1 modulates the tissue-specific expression patterns of BAS1 and SOB7 in leaves and siliques.

Fig. S3. Compared with Col-0, *ataf2-2* seedlings did not show significant changes of *CCA1* expression in either continuous light or darkness.

Acknowledgements

This research was supported by the United States National Science Foundation project #1656265 (to MMN) and by the USDA National Institute of Food and Agriculture, Hatch Umbrella Project #1015621 (to MMN). The authors would like to thank Dr James N. Culver (University of Maryland) for providing the p*ATAF2*::GUS construct. We also thank Dr Gaganjot Sidhu and Shahbaz Ahmad in the Neff Lab for their critical review and comments on this manuscript. The authors have no conflict of interest to declare.

References

Arvidsson S, Kwasniewski M, Riaño-Pachón DM, Mueller-Roeber B. 2008. QuantPrime—a flexible tool for reliable high-throughput primer design for quantitative PCR. BMC Bioinformatics **9**, 465.

Asami T, Min YK, Nagata N, Yamagishi K, Takatsuto S, Fujioka S, Murofushi N, Yamaguchi I, Yoshida S. 2000. Characterization of brassinazole, a triazole-type brassinosteroid biosynthesis inhibitor. Plant Physiology **123**, 93–100.

Belkhadir Y, Jaillais Y, Epple P, Balsemão-Pires E, Dangl JL, Chory J. 2012. Brassinosteroids modulate the efficiency of plant immune responses to microbe-associated molecular patterns. Proceedings of the National Academy of Sciences, USA **109**, 297–302.

Bell EM, Lin WC, Husbands AY, Yu L, Jaganatha V, Jablonska B, Mangeon A, Neff MM, Girke T, Springer PS. 2012. *Arabidopsis* lateral organ boundaries negatively regulates brassinosteroid accumulation to limit growth in organ boundaries. Proceedings of the National Academy of Sciences, USA **109**, 21146–21151.

Chae K, Isaacs CG, Reeves PH, Maloney GS, Muday GK, Nagpal P, Reed JW. 2012. *Arabidopsis* SMALL AUXIN UP RNA63 promotes hypocotyl and stamen filament elongation. The Plant Journal **71**, 684–697.

Choi S, Cho YH, Kim K, Matsui M, Son SH, Kim SK, Fujioka S, Hwang I. 2013. BAT1, a putative acyltransferase, modulates brassinosteroid levels in *Arabidopsis*. The Plant Journal **73**, 380–391.

Delessert C, Kazan K, Wilson IW, Van Der Straeten D, Manners J, Dennis ES, Dolferus R. 2005. The transcription factor ATAF2 represses the expression of pathogenesis-related genes in *Arabidopsis*. The Plant Journal **43**, 745–757.

Deplancke B, Dupuy D, Vidal M, Walhout AJ. 2004. A gateway-compatible yeast one-hybrid system. Genome Research **14**, 2093–2101.

Deplancke B, Vermeirssen V, Arda HE, Martinez NJ, Walhout AJ. 2006. Gateway-compatible yeast one-hybrid screens. Cold Spring Harbor Protocols doi: 10.1101/pdb.prot4590.

Favero DS, Jacques CN, Iwase A, Le KN, Zhao J, Sugimoto K, Neff MM. 2016. SUPPRESSOR OF PHYTOCHROME B4-#3 represses genes associated with auxin signaling to modulate hypocotyl growth. Plant Physiology **171**, 2701–2716.

Favero DS, Le KN, Neff MM. 2017. Brassinosteroid signaling converges with SUPPRESSOR OF PHYTOCHROME B4-#3 to influence the expression of *SMALL AUXIN UP RNA* genes and hypocotyl growth. The Plant Journal **89**, 1133–1145.

Fujiwara S, Oda A, Yoshida R, *et al*. 2008. Circadian clock proteins LHY and CCA1 regulate SVP protein accumulation to control flowering in *Arabidopsis*. The Plant Cell **20**, 2960–2971.

Green RM, Tobin EM. 1999. Loss of the circadian clock-associated protein 1 in *Arabidopsis* results in altered clock-regulated gene expression. Proceedings of the National Academy of Sciences, USA **96**, 4176–4179.

Guo Z, Fujioka S, Blancaflor EB, Miao S, Gou X, Li J. 2010. TCP1 modulates brassinosteroid biosynthesis by regulating the expression of the key biosynthetic gene DWARF4 in *Arabidopsis thaliana*. The Plant Cell **22**, 1161–1173.

Harmer SL, Kay SA. 2005. Positive and negative factors confer phase-specific circadian regulation of transcription in *Arabidopsis*. The Plant Cell **17**, 1926–1940.

He JX, Gendron JM, Sun Y, Gampala SS, Gendron N, Sun CQ, Wang ZY. 2005. BZR1 is a transcriptional repressor with dual roles in brassinosteroid homeostasis and growth responses. Science **307**, 1634–1638.

Huh SU, Lee SB, Kim HH, Paek KH. 2012. ATAF2, a NAC transcription factor, binds to the promoter and regulates NIT2 gene expression involved in auxin biosynthesis. Molecules and Cells **34**, 305–313.

Husar S, Berthiller F, Fujioka S, *et al*. 2011. Overexpression of the *UGT73C6* alters brassinosteroid glucoside formation in *Arabidopsis thaliana*. BMC Plant Biology **11**, 51.

Kamioka M, Takao S, Suzuki T, Taki K, Higashiyama T, Kinoshita T, Nakamichi N. 2016. Direct repression of evening genes by CIRCADIAN CLOCK-ASSOCIATED1 in the *Arabidopsis* circadian clock. The Plant Cell **28**, 696–711.

Kim HB, Kwon M, Ryu H, Fujioka S, Takatsuto S, Yoshida S, An CS, Lee I, Hwang I, Choe S. 2006. The regulation of *DWARF4* expression is likely a critical mechanism in maintaining the homeostasis of bioactive brassinosteroids in *Arabidopsis*. Plant Physiology **140**, 548–557.

Kleinow T, Himbert S, Krenz B, Jeske H, Koncz C. 2009. NAC domain transcription factor ATAF1 interacts with SNF1-related kinases and silencing of its subfamily causes severe developmental defects in *Arabidopsis*. Plant Science **177**, 360–370.

Li G, Siddiqui H, Teng Y, *et al*. 2011. Coordinated transcriptional regulation underlying the circadian clock in *Arabidopsis*. Nature Cell Biology **13**, 616–622.

Marsolais F, Boyd J, Paredes Y, Schinas AM, Garcia M, Elzein S, Varin L. 2007. Molecular and biochemical characterization of two brassinosteroid sulfotransferases from *Arabidopsis*, AtST4a (At2g14920) and AtST1 (At2g03760). Planta **225**, 1233–1244.

Michael TP, McClung CR. 2002. Phase-specific circadian clock regulatory elements in *Arabidopsis*. Plant Physiology **130**, 627–638.

Nagahage ISP, Sakamoto S, Nagano M, Ishikawa T, Kawai-Yamada M, Mitsuda N, Yamaguchi M. 2018. An NAC domain transcription factor ATAF2 acts as transcriptional activator or repressor dependent on promoter context. Plant Biotechnology **35**, 285–289.

Nagel DH, Doherty CJ, Pruneda-Paz JL, Schmitz RJ, Ecker JR, Kay SA. 2015. Genome-wide identification of CCA1 targets uncovers an expanded clock network in *Arabidopsis*. Proceedings of the National Academy of Sciences, USA **112**, E4802–E4810.

Nakamura M, Satoh T, Tanaka S, Mochizuki N, Yokota T, Nagatani A. 2005. Activation of the cytochrome P450 gene, *CYP72C1*, reduces the levels of active brassinosteroids *in vivo*. Journal of Experimental Botany **56**, 833–840.

Neff MM, Nguyen SM, Malancharuvil EJ, *et al*. 1999. BAS1: a gene regulating brassinosteroid levels and light responsiveness in *Arabidopsis*. Proceedings of the National Academy of Sciences, USA **96**, 15316–15323.

Nolan T, Chen J, Yin Y. 2017. Cross-talk of brassinosteroid signaling in controlling growth and stress responses. The Biochemical Journal **474**, 2641–2661.

Pan Y, Michael TP, Hudson ME, Kay SA, Chory J, Schuler MA. 2009. Cytochrome P450 monooxygenases as reporters for circadian-regulated pathways. Plant Physiology **150**, 858–878.

Peng H, Zhao J, Neff MM. 2015. ATAF2 integrates *Arabidopsis* brassinosteroid inactivation and seedling photomorphogenesis. Development **142**, 4129–4138.

Poppenberger B, Fujioka S, Soeno K, *et al*. 2005. The UGT73C5 of *Arabidopsis thaliana* glucosylates brassinosteroids. Proceedings of the National Academy of Sciences, USA **102**, 15253–15258.

Poppenberger B, Rozhon W, Khan M, Husar S, Adam G, Luschnig C, Fujioka S, Sieberer T. 2011. CESTA, a positive regulator of brassinosteroid biosynthesis. The EMBO Journal **30**, 1149–1161.

Pruneda-Paz JL, Breton G, Para A, Kay SA. 2009. A functional genomics approach reveals CHE as a component of the *Arabidopsis* circadian clock. Science **323**, 1481–1485.

Roh H, Jeong CW, Fujioka S, Kim YK, Lee S, Ahn JH, Choi YD, Lee JS. 2012. Genetic evidence for the reduction of brassinosteroid levels by a BAHD acyltransferase-like protein in *Arabidopsis*. Plant Physiology **159**, 696–709.

Sandhu KS, Hagely K, Neff MM. 2012. Genetic interactions between brassinosteroid-inactivating P450s and photomorphogenic photoreceptors in *Arabidopsis thaliana.* G3 **2**, 1585–1593.

Sandhu KS, Neff MM. 2013. The *Arabidopsis* gene *ATST4a* in not a typical brassinosteroid catabolic gene. Plant Signaling & Behavior **8**, doi: 10.4161/psb.26847.

Savaldi-Goldstein S, Peto C, Chory J. 2007. The epidermis both drives and restricts plant shoot growth. Nature **446**, 199–202.

Schaffer R, Ramsay N, Samach A, Corden S, Putterill J, Carré IA, Coupland G. 1998. The late elongated hypocotyl mutation of *Arabidopsis* disrupts circadian rhythms and the photoperiodic control of flowering. Cell **93**, 1219–1229.

Schneider CA, Rasband WS, Eliceiri KW. 2012. NIH Image to ImageJ: 25 years of image analysis. Nature Methods **9**, 671–675.

Schneider K, Breuer C, Kawamura A, *et al*. 2012. *Arabidopsis* PIZZA has the capacity to acylate brassinosteroids. PLoS One **7**, e46805.

Shahnejat-Bushehri S, Tarkowska D, Sakuraba Y, Balazadeh S. 2016. *Arabidopsis* NAC transcription factor JUB1 regulates GA/BR metabolism and signalling. Nature Plants **2**, 16013.

Spartz AK, Lee SH, Wenger JP, Gonzalez N, Itoh H, Inzé D, Peer WA, Murphy AS, Overvoorde PJ, Gray WM. 2012. The SAUR19 subfamily of *SMALL AUXIN UP RNA* genes promote cell expansion. The Plant Journal **70**, 978–990.

Symons GM, Reid JB. 2004. Brassinosteroids do not undergo long-distance transport in pea. Implications for the regulation of endogenous brassinosteroid levels. Plant Physiology **135**, 2196–2206.

Symons GM, Ross JJ, Jager CE, Reid JB. 2008. Brassinosteroid transport. Journal of Experimental Botany **59**, 17–24.

Takasaki H, Maruyama K, Takahashi F, Fujita M, Yoshida T, Nakashima K, Myouga F, Toyooka K, Yamaguchi-Shinozaki K, Shinozaki K. 2015. SNAC-As, stress-responsive NAC transcription factors, mediate ABA-inducible leaf senescence. The Plant Journal **84**, 1114–1123.

Takahashi N, Nakazawa M, Shibata K, Yokota T, Ishikawa A, Suzuki K, Kawashima M, Ichikawa T, Shimada H, Matsui M. 2005. *shk1-D*, a dwarf *Arabidopsis* mutant caused by activation of the *CYP72C1* gene, has altered brassinosteroid levels. The Plant Journal **42**, 13–22.

Tanaka K, Asami T, Yoshida S, Nakamura Y, Matsuo T, Okamoto S. 2005. Brassinosteroid homeostasis in *Arabidopsis* is ensured by feedback expressions of multiple genes involved in its metabolism. Plant Physiology **138**, 1117–1125.

Teytelman L, Thurtle DM, Rine J, van Oudenaarden A. 2013. Highly expressed loci are vulnerable to misleading ChIP localization of multiple unrelated proteins. Proceedings of the National Academy of Sciences, USA **110**, 18602–18607.

Thornton LE, Rupasinghe SG, Peng H, Schuler MA, Neff MM. 2010. *Arabidopsis* CYP72C1 is an atypical cytochrome P450 that inactivates brassinosteroids. Plant Molecular Biology **74**, 167–181.

Thornton LE, Peng H, Neff MM. 2011. Rice CYP734A cytochrome P450s inactivate brassinosteroids in *Arabidopsis*. Planta **234**, 1151–1162.

Turk EM, Fujioka S, Seto H, Shimada Y, Takatsuto S, Yoshida S, Denzel MA, Torres QI, Neff MM. 2003. CYP72B1 inactivates brassinosteroid hormones: an intersection between photomorphogenesis and plant steroid signal transduction. Plant Physiology **133**, 1643–1653.

Turk EM, Fujioka S, Seto H, *et al*. 2005. BAS1 and SOB7 act redundantly to modulate *Arabidopsis* photomorphogenesis via unique brassinosteroid inactivation mechanisms. The Plant Journal **42**, 23–34.

Wang H, Zhu Y, Fujioka S, Asami T, Li J, Li J. 2009. Regulation of *Arabidopsis* brassinosteroid signaling by atypical basic helix–loop–helix proteins. The Plant Cell **21**, 3781–3791.

Wang M, Liu X, Wang R, Li W, Rodermel S, Yu F. 2012. Overexpression of a putative *Arabidopsis* BAHD acyltransferase causes dwarfism that can be rescued by brassinosteroid. Journal of Experimental Botany **63**, 5787–5801.

Wang X, Culver JN. 2012. DNA binding specificity of ATAF2, a NAC domain transcription factor targeted for degradation by *Tobacco mosaic virus*. BMC Plant Biology **12**, 157.

Wang X, Goregaoker SP, Culver JN. 2009. Interaction of the Tobacco mosaic virus replicase protein with a NAC domain transcription factor is associated with the suppression of systemic host defenses. Journal of Virology **83**, 9720–9730.

Wang ZY, Kenigsbuch D, Sun L, Harel E, Ong MS, Tobin EM. 1997. A Myb-related transcription factor is involved in the phytochrome regulation of an *Arabidopsis Lhcb* gene. The Plant Cell **9**, 491–507.

Wang ZY, Tobin EM. 1998. Constitutive expression of the CIRCADIAN CLOCK ASSOCIATED 1 (CCA1) gene disrupts circadian rhythms and suppresses its own expression. Cell **93**, 1207–1217.

Wei Z, Yuan T, Tarkowská D, Kim J, Nam HG, Novák O, He K, Gou X, Li J. 2017. Brassinosteroid biosynthesis is modulated via a transcription factor cascade of COG1, PIF4, and PIF5. Plant Physiology **174**, 1260–1273.

Yakir E, Hilman D, Kron I, Hassidim M, Melamed-Book N, Green RM. 2009. Posttranslational regulation of CIRCADIAN CLOCK ASSOCIATED1 in the circadian oscillator of *Arabidopsis*. Plant Physiology **150**, 844–857.

Ye H, Li L, Guo H, Yin Y. 2012. MYBL2 is a substrate of GSK3-like kinase BIN2 and acts as a corepressor of BES1 in brassinosteroid signaling pathway in *Arabidopsis*. Proceedings of the National Academy of Sciences, USA **109**, 20142–20147.

Youn JH, Kim MK, Kim EJ, Son SH, Lee JE, Jang MS, Kim TW, Kim SK. 2016. ARF7 increases the endogenous contents of castasterone through suppression of *BAS1* expression in *Arabidopsis thaliana*. Phytochemistry **122**, 34–44.

Yuan T, Fujioka S, Takatsuto S, Matsumoto S, Gou X, He K, Russell SD, Li J. 2007. *BEN1*, a gene encoding a dihydroflavonol 4-reductase (DFR)-like protein, regulates the levels of brassinosteroids in *Arabidopsis thaliana*. The Plant Journal **51**, 220–233.

Zhang Z, Xu L. 2018. *Arabidopsis* BRASSINOSTEROID INACTIVATOR2 is a typical BAHD acyltransferase involved in brassinosteroid homeostasis. Journal of Experimental Botany **69**, 1925–1941.

Zhao B, Li J. 2012. Regulation of brassinosteroid biosynthesis and inactivation. Journal of Integrative Plant Biology **54**, 746–759.

Zhao J, Favero DS, Peng H, Neff MM. 2013. *Arabidopsis thaliana* AHL family modulates hypocotyl growth redundantly by interacting with each other via the PPC/DUF296 domain. Proceedings of the National Academy of Sciences, USA **110**, E4688–E4697.

Zheng H, Zhang F, Wang S, Su Y, Ji X, Jiang P, Chen R, Hou S, Ding Y. 2018. MLK1 and MLK2 coordinate RGA and CCA1 activity to regulate hypocotyl elongation in *Arabidopsis thaliana*. The Plant Cell **30**, 67–82.

Zhu JY, Sae-Seaw J, Wang ZY. 2013. Brassinosteroid signalling. Development **140**, 1615–1620.

Zhu W, Wang H, Fujioka S, Zhou T, Tian H, Tian W, Wang X. 2013. Homeostasis of brassinosteroids regulated by DRL1, a putative acyltransferase in *Arabidopsis*. Molecular Plant **6**, 546–558.